Available online at BCREC website: https://bcrec.id

Bulletin of Chemical Reaction Engineering & Catalysis, 18 (2) 2023, 222-237

Research Article

High Acidity and Low Carbon-Coke Formation Affinity of Co-Ni/ZSM-5 Catalyst for Renewable Liquid Fuels Production through Simultaneous Cracking-Deoxygenation of Palm Oil

I. Istadi[1,2,*], Teguh Riyanto[1,2], Didi Dwi Anggoro[2], Cokorda Satrya Pramana[2], Amalia Rizqi Ramadhani[2]

[1]Laboratory of Plasma-Catalysis (R3.5), Center of Research and Services - Diponegoro University (CORES-DU), Integrated Laboratory, Universitas Diponegoro, Semarang 50275, Indonesia.
[2]Department of Chemical Engineering, Faculty of Engineering, Universitas Diponegoro, Semarang 50275, Indonesia.

Received: 12th April 2023; Revised: 18th May 2023; Accepted: 18th May 2023
Available online: 20th May 2023; Published regularly: July 2023

Abstract

This study investigates the effect of chemically doped Co and Ni metals on ZSM-5 catalyst with respect to the catalysts' characteristics and performance for palm oil cracking. Some characterization methods have been conducted to identify the physicochemical properties of the synthesized catalysts, including X-ray diffraction (XRD), Scanning Electron Microscopy (SEM), N_2-physisorption, NH_3- and CO_2-probed Temperature Programmed Desorption (NH_3-TPD and CO_2-TPD) methods. The deposited carbon-coke on the spent catalysts is analysed using simultaneous thermal gravimetric–differential scanning calorimetry (TG-DTG-DSC) analysis. The performance of catalysts was evaluated on palm oil cracking process in a continuous fixed-bed catalytic reactor at 450 °C. To determine the liquid product composition functional group and components, we used Attenuated Total Reflectance Fourier-transform Infrared Spectroscopy (ATR-FTIR) and batch distillation methods, respectively. We found that the Co metal chemically-doped on Ni/SM-5 catalyst, resulting the increase in the catalysts acidity and the decrease in catalysts basicity. The conversion of palm oil increases as the increase of the ratio of catalysts' acidity to basicity. The highest triglyceride conversion (76.5%) was obtained on the 3Co-Ni/ZSM-5 with the yield of gasoline, kerosene, and diesel of 2.61%, 4.38%, and 61.75%, respectively. It was also found that the chemically doping Co metal on Ni/ZSM-5 catalyst decreased carbon-coke formation due to the low catalysts' basicity. Overall, it is proven that the combination of Co and Ni, which chemically doped, on ZSM-5 catalyst has a good activity in palm oil conversion with low carbon-coke formation affinity and high acidity of catalyst.

Keywords: Palm oil; Carbon-Coke formation; Cracking; Deoxygenation; Acidity; Basicity; Chemically doped

How to Cite: I. Istadi, T. Riyanto, D.D. Anggoro, C.S. Pramana, A.R. Ramadhani (2023). High Acidity and Low Carbon-Coke Formation Affinity of Co-Ni/ZSM-5 Catalyst for Renewable Liquid Fuels Production through Simultaneous Cracking-Deoxygenation of Palm Oil. *Bulletin of Chemical Reaction Engineering & Catalysis*, 18(2), 222-237 (doi: 10.9767/bcrec.17974)

Permalink/DOI: https://doi.org/10.9767/bcrec.17974

1. Introduction

In Indonesia, biofuels production development has been conducted and implemented by producing biodiesel from palm oil and other vegetable oils through a transesterification reaction. However, this reaction only produces one type of biofuels, which is biodiesel from fatty acid methyl ester (FAME). The properties of FAME highly depend on the feedstock properties [1,2] and typically has a high viscosity, oxygen content, and unsaturated acid content,

* Corresponding Author.
Email: istadi@che.undip.ac.id (I. Istadi)

causing biodiesel to have a low heating value as well as low oxidation stability [3]. The utilization of FAME in modern diesel engines can cause some technical problems, such as filter blockage and engine corrosion in long-term operation, due to its high oxygen content [4,5]. Therefore, it is necessary to convert vegetable oil into more diverse biofuels as alternative sources of diesel, kerosene, and gasoline.

One of the efforts to produce diverse biofuels as alternative source of diesel, kerosene, and gasoline is conducted through the catalytic cracking process of palm oil or other vegetable oils [6]. Therefore, the catalytic cracking process has more potential to be developed because it produces a diverse biofuels product and renewable. Several researchers have conducted the catalytic cracking of palm oil to biofuels using acid catalysts because they have better activity than base catalysts. Zeolite-based catalysts, such as HY, ZSM-5, and MCM-41, are the most-developed acid catalysts [7–11]. Gurdeep Singh *et al*. [9] used ZSM-5 catalyst to convert linoleic acid, as a model compound, into biogasoline through the cracking process. The ZSM-5 can increase the aromatic compounds, which can increase the octane number of biogasoline, although a high aromatic content may be released as benzene compounds which is proven as toxic compounds [9]. ZSM-5 catalyst has been utilized as catalyst for cracking process due to its good porosity nature and supporting aromatization [12]. In addition, the modification of the zeolite catalysts using transition metals can improve the performance of catalysts to produce biofuels because of changes in their acidity or generated acid sites. Riyanto *et al*. [12] improved the ZSM-5 catalyst using some metal oxides, where the Lewis acid site of the catalyst was increased after Co impregnation, resulting in the increase of biofuels product. Istadi *et al*. [11] utilized Ni and Co to modify HY catalyst for palm oil cracking, although it did not significantly change the yield of liquid fuels; however, the hydrocarbons selectivity was massively increased. Nevertheless, the impregnation of Ni on HY led to increasing carbon-coke formation. Some studies also reported that Ni has a high affinity leading to carbon-coke formation [9,11,13]. Botas *et al*. [13] reported that the Mo-modified nanocrystalline ZSM-5 zeolite could increase the aromatic compounds on the catalytic conversion of rapeseed oil. Haji Morni *et al*. [14] modified the ZSM-5 using Ni and Mo for the co-pyrolysis of sewage sludge-sawdust. It was reported that MoO_3 could reduce the aromatic compounds. However, incorporating NiO with MoO_3 could massively increase the aromatic compounds selectivity as well as the oxygenated compounds [14].

Based on the previous studies, the main concern in the proposed catalyst modification is to improve the catalytic activity of catalysts towards biofuels production, particularly due to improved high acidity of catalyst, without reducing the catalyst porosity significantly. However, the side reaction, especially carbon-coke formation, should be considered to be avoided or decreased. However, carbon-coke formation cannot be avoided in the cracking process, therefore, it can be minimized through catalyst modification. With respect to the requirement, the present research is driven to design a catalyst that not only can actively support the cracking process of palm oil to biofuel due to increasing the catalyst acidity without reducing porosity significantly, but also has low carbon-coke formation affinity. In addition, the deoxygenation process is less discussed in the cracking process of vegetable oils in some literatures. Therefore, this study investigates the effect of chemically doped Co and Ni metals on the Ni/ZSM-5 catalyst with respect to improving the liquid fuels formation due to improved catalyst acidity without reduced catalyst porosity and lowering carbon-coke formation affinity during the cracking-deoxygenation process palm oil to biofuels.

2. Materials and Methods

2.1 Materials

Commercial ZSM-5 (CBV 8014) catalyst was obtained from Zeolyst International. Nickel(II) nitrate hexahydrate ($Ni(NO_3)_2.6H_2O$) and Cobalt(II) nitrate hexahydrate ($Co(NO_3)_2.6H_2O$) were used as the precursors for catalysts synthesis. Both precursors were obtained from Merk. In order to test the performance of catalysts in the catalytic cracking process, palm oil from was used as the feedstock. Nitrogen (N_2) gas (UHP) was used as the flushing agent before cracking process.

2.2 Catalysts Synthesis

The catalysts (Co-Ni/ZSM-5) were synthesized using wet impregnation with considering only chemically doped of Co and Ni metals on ZSM-5. Firstly, Ni/ZSM-5 was synthesized by immersing approximately 20 g of ZSM-5 in the Ni solution (200 mL). The Ni metal was adjusted so that the impregnated Ni was 15 wt% on the catalyst. The slurry was then stirred (300 rpm) for 12 h and then filtered in order to only

consider chemically doping. The obtained solid was dried at 110 °C overnight and calcined at 550 °C for 4 h. The obtained catalyst was denoted as Ni/ZSM-5 catalyst. In order to synthesized Co-Ni/ZSM-5 catalysts, the synthesized Ni/ZSM-5 catalyst was immersed in the Co solution (200 mL) and stirred (300 rpm) for 12 h and then filtered to only consider chemically doping. Thus, the targeted Ni and Co contents was only chemically adsorbed on the ZSM-5 catalyst, excluding the bulk phase of NiO and/or CoO on the surface ZSM-5. The amount of Co on the catalyst was varied at 3, 6, and 10%wt. The obtained slurry was dried at 110 °C overnight and calcined at 550 °C for 4 h. The catalysts were denoted as 3Co-Ni/ZSM-5, 6Co-ZSM-5, and 10Co-ZSM-5 with respect to Co amount of 3, 6, and 10%, respectively. The catalysts powder was palleted and crushed so that the catalysts size is 1-1.8 mm.

2.4 Catalysts Characterizations Methods

The synthesized catalysts were characterized using several analytical methods. The crystal structure of catalysts was investigated using X-ray diffraction analysis (XRD). The diffraction pattern of Cu-Kα radiation (λ = 1.54 Å) was collected at 2θ of 5–90° with a scanning speed of 5° min^{-1} using Shimadzu 7000. The surface morphology of the synthesized catalysts was investigated using Scanning Electron Microscopy (SEM) method. Further evaluation of SEM analysis was performed using ImageJ to estimate the average particle size. The N_2-physisorption was performed using ChemBET PULSAR (Quantachrome) to estimate the surface area and the pore size distributions of the synthesized catalysts. Prior to the N_2-adsorption, the catalysts were degassed at 300 °C for 3 h. The acidity and basicity strengths of catalysts were evaluated using Temperature Programmed Desorption (TPD). NH_3 was used as the probe molecule in the acidity test, while CO_2 was used as the probe molecule in the basicity test. The adsorption of NH_3 was conducted at 100 °C and the desorption was conducted from 100 °C to 900 °C with a heating rate of 10 °C/min and then the heating was hold for 5 min. In the basicity analysis, the adsorption of CO_3 was conducted at room temperature and the desorption was conducted from room temperature to 900 °C with a heating rate of 10 °C/min and then the heating was hold for 5 min. Both acidity and basicity analyses were conducted using Autochem II Micromeritics. In order to investigate the coke formation, the spent catalysts were analysed using thermal analysis using Simultaneous Thermal Analyser (STA200RV Hitachi) using Thermo-Gravimetry (TG), Derivative Thermo Gravimetry (DTG), and Differential Scanning Calorimetry (DSC). During the thermal analysis process, the heating rate was 10 °C/min in air atmosphere (flow = 100 mL/min). Prior to the TG analysis, the spent catalysts were washed using n-hexane through Soxhlet extraction method.

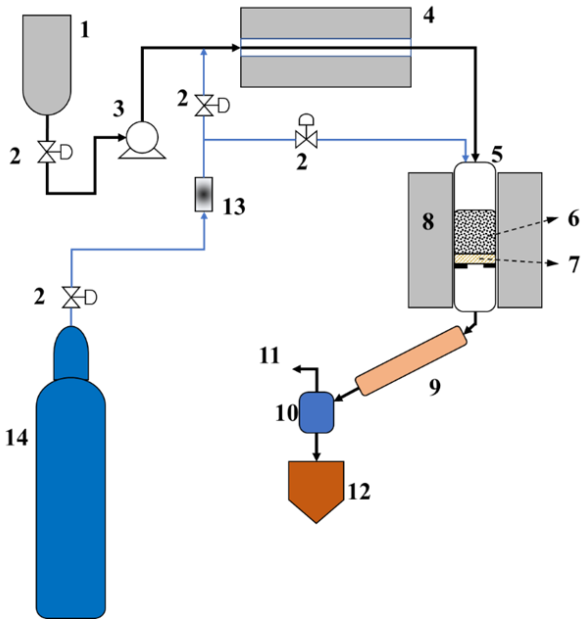

Figure 1. Schematic diagram of experimental set up of the continuous catalytic cracking process: (1) Palm oil feedstock tank, (2) Gate valve, (3) Peristaltic pump, (4) Preheater, (5) Reactor tube, (6) Catalysts packing, (7) Glass wool, (8) Electric heating furnace as reactor heater, (9) Condenser, (10) Gas-liquid separator, (11) Gas by product, (12) Liquid fuels product, (13) Gas flowmeter, and (14) Nitrogen gas tank.

2.5 Catalysts Performance Test

The continuous cracking reaction process for palm oil served as a test and evaluation ground for the catalysts' performance. The schematic diagram of the experimental setup for the palm oil cracking process is shown in Figure 1. The reactor was a stainless-steel pipe with an internal diameter of 2.54 cm. Approximately, 5 g of catalyst was put in the reactor, which was supported by glass wool. Prior to the reaction, oxygen that had become trapped in the experimental setup was flushed out by nitrogen flow at a rate of 100 mL/min for 30 min. A peristaltic pump was used to feed the reactor with palm oil from the tank. The flow rate of palm oil was adjusted to achieve a weight hourly space velocity (WHSV) of 0.365 min^{-1}. The

cracking process was carried out at 450 °C. In the condenser, the cracking products were condensed. The liquid products (condensed chemicals) and volatile compounds were divided. After the process achieved a steady state, the liquid products were collected for 2 h. The yield of OLP and gas and coke were calculated using Equation (1) and were utilized to assess the effectiveness of catalysts for cracking palm oil into biofuels.

$$Y_i\ (\%) = \frac{m_i}{m_{feed}} \times 100 \quad (1)$$

In this equation, Y_i represents the yield of component (liquid product or gas and coke), m_i stands for the mass of liquid product or gas and coke, and m_{feed} represents the total mass of palm oil that was fed.

2.6 Composition Analysis of Liquid Product

In order to investigate the functional group in the liquid products, the liquid products were analysed using ATR-FTIR Spectroscopy (Attenuated Total Reflectance Fourier-transform Infrared Spectroscopy). The FT-IR spectra were collected at wave number of 400–4000 cm^{-1} using Perkin-Elmer UATR Spectrum Two. The conversion of palm oil (triglyceride) was calculated by applying the area of absorption band of the carbonyl group (1745 cm^{-1}) using Equation (2), where $A_{1745\ palm\ oil}$ represents the area of absorption band at 1745 cm^{-1} of palm oil and $A_{1745\ liquid\ fuels}$ represents the area of absorption band at 1745 cm^{-1} of liquid products.

$$Conversion\ (\%) = \frac{A_{1745\ palm\ oil} - A_{1745\ liquid\ fuels}}{A_{1745\ palm\ oil}} \times 100 \quad (2)$$

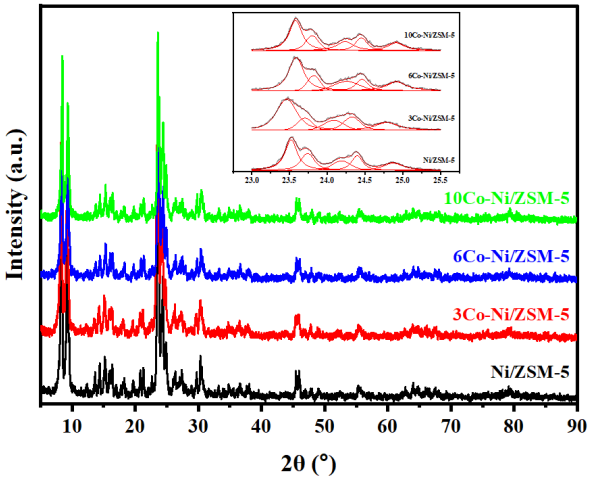

Figure 2. XRD patterns of Ni/ZSM-5, 3Co-Ni/ZSM-5, 6Co-Ni/ZSM-5, and 10Co-Ni/ZSM-5.

In order to investigate the composition in the liquid products, a batch distillation was performed. The liquid products were distilled from room temperature to 370 °C. The distillate at room temperature to 205 °C was assigned to the gasoline fraction, the distillate at 205-310 °C was collected as kerosene fraction, and the distillate at 310-370 °C was collected was diesel fraction. The yield of gasoline, kerosene, and diesel was calculated using Equation (3).

$$Y_j\ (\%) = \frac{m_j}{m_f} \times Y_{liquid\ product} \times 100 \quad (3)$$

In this equation, Y_j represents the yield of component j (gasoline, kerosene, or diesel), m_j represents the mass of component j, m_f represents the mass of liquid product that was fed to the distillation set, and $Y_{liquid\ product}$ represents the yield of liquid product.

3. Results and Discussions

3.1 Catalysts Characterizations

3.1.1 Crystal structure of catalysts

The crystal structure of the synthesized catalysts was investigated using XRD analysis. The diffraction patterns of the catalysts were collected at 2θ of 5–90°. Figure 2 depicts the diffraction patterns of Ni/ZSM-5, 3Co-Ni/ZSM-5, 6Co-Ni/ZSM-5, and 10Co-Ni/ZSM-5. As shown in Figure 2, the all catalysts exhibit orthorhombic MFI structure due to the appearance of the intense peaks at 2θ = 7.95°, 8.89°, 23.49°, 23.71°, 24.13°, 24.35°, and 24.83°, corresponding to the (101), (020), (501), (051), (151), (303) and (133) planes (COD reference code: 96-154-0268), respectively. It is found that the characteristic quintet of MFI structure appears at 2θ = 23–25.5° (inset figure in Figure 2). Therefore, it is suggested that all catalysts have MFI structure as the main crystal structure.

Based on the XRD patterns, the diffraction patterns of the catalysts are not changed after metals impregnation. It indicates that the crystal structures of the catalysts are not changed significantly. As mentioned before, the main crystal structure of the catalysts is MFI structure. Therefore, it is suggested that the MFI structure is not changed significantly by the chemically doped impregnation method of NiO and CoO, owing to only small amount of NiO and CoO doped on the catalyst surface due to only chemically doped of metals was considered. Therefore, diffraction patterns of the catalysts are not significantly appeared.

3.1.2 Textural properties of catalysts

The textural characteristics of supports have a significant impact on the catalytic performance. In this study, the textural properties of the catalysts were characterized using N_2-physisorption method. The N_2-sorption isotherms of the catalysts are presented in Figure 3. It is shown in Figure 3 that the sorption isotherms of all catalysts are similar which shows a rapid increase of N_2 adsorption at a low relative pressure ($p/p° < 0.01$). This intense adsorption is attributed to the micropore filling, indicating that all catalysts have micropores. It can also be seen that the sorption isotherm curves of the catalysts, based on IUPAC classification, are classified as sorption isotherm Type IV which is accompanied with hysteresis loop. Sorption isotherm Type IV is generally produced from mesoporous materials [15]. In addition, this hysteresis loop is classified as Type H4 loop. Thommes *et al.* [15] stated that a more pronounced uptake at low $p/p°$ being associated with the micropores filling. Therefore, it can be concluded that the catalysts have both micropores and mesopores.

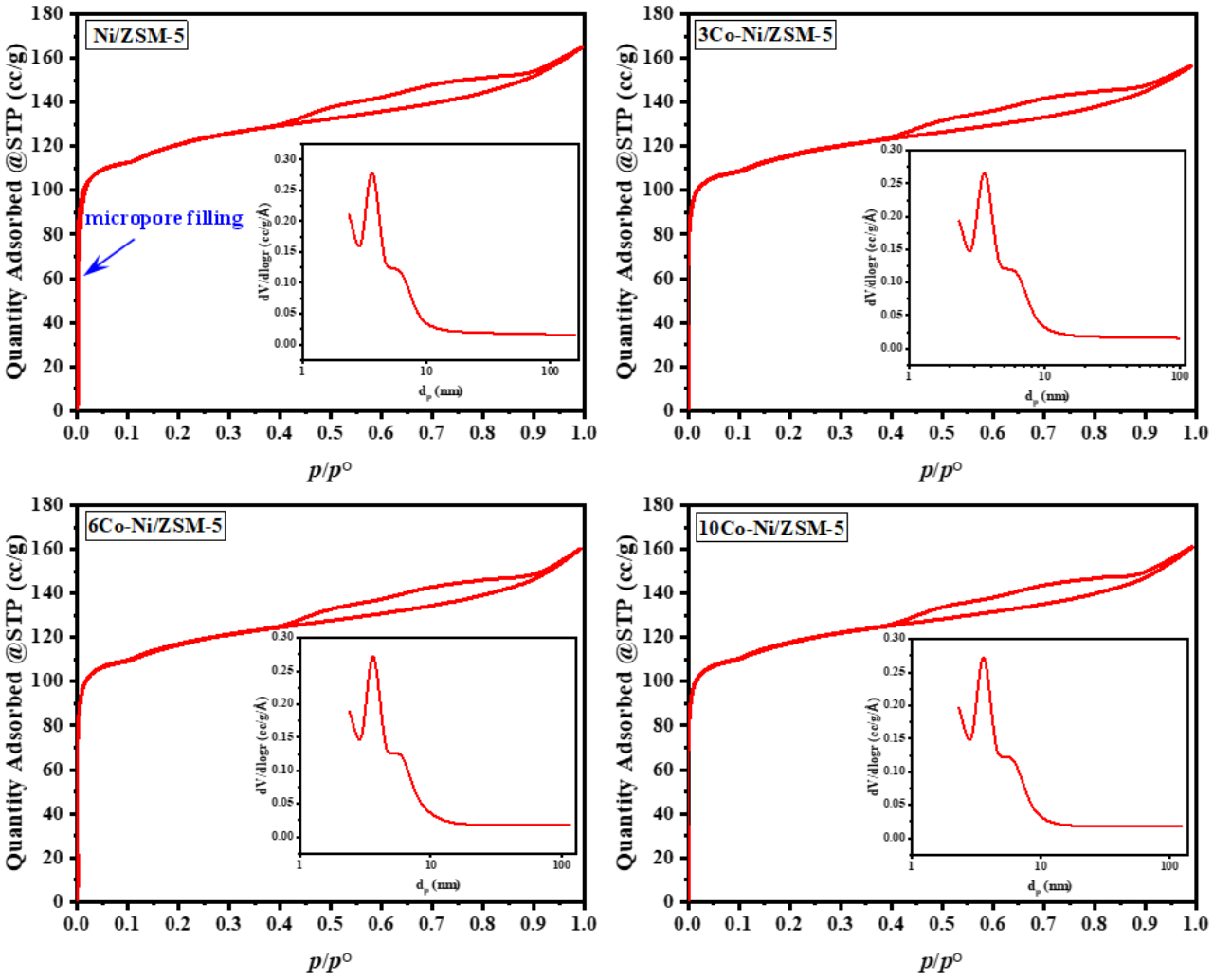

Figure 3. N_2-sorption isotherm and pore size distribution of catalysts.

Table 1. Textural properties of catalysts.

Catalysts	S_{BET}* (m²/g)	S_{ext}‡ (m²/g)	S_{micro}‡ (m²/g)	V_p⁂ (cc/g)	V_{micro}‡ (cc/g)	d_p‡ (nm)
Ni/ZSM-5	374	180	194	0.255	0.108	3.64
3Co-Ni/ZSM-5	359	153	206	0.242	0.111	3.60
6Co-Ni/ZSM-5	360	154	206	0.248	0.112	3.62
10Co-Ni/ZSM-5	363	156	207	0.249	0.113	3.60

*Based on BET method; ‡Based on *t*-plot; ⁂Total pore volume at $p/p° = 0.99$; ‡Average pore size using BJH method based on N_2-desorption.

Based on the sorption isotherm curves, the addition of Co metal on Ni/ZSM-5 catalyst does not significantly change the textural properties of the catalysts. Therefore, some parameters, such as surface area, pore size and pore volume, need to be evaluated further. As can be seen in Table 1, the surface area of the catalyst decreased slightly after the addition of Co metal which is caused by the pore blocking by the chemically doped metal and is also proven by the decrease slightly in the pore volume and average pore size of the catalyst (Table 1). However, the micropore volume of the catalyst increases as the increase in Co metal addition. Therefore, it can be concluded that the slight decrease in surface area, pore volume, and pore size of catalysts is caused by the partial blocking of mesopores by metal. The mesopores of catalysts are partially blocked by metal so that the pores become narrower leading to increased micropore volume and micropore surface area. This fact confirms that the chemically doped Co metal has been impregnated on the surface of catalyst even though it was not detected in XRD analysis.

The surface morphology of the catalysts was observed using SEM analysis. The surface morphology of the catalysts is depicted in Figure 4. It is presented that the surface morphology of the catalyst does not change significantly after the addition of Co metal on the catalyst, because of only small Ni and Co is chemically doped on the catalyst surface. Moreover, the catalysts' particles size also looks as if not changed significantly. By utilizing normal distribution, the average particles sizes of Ni/ZSM-5, 3Co-Ni/ZSM-5, 6Co-Ni/ZSM-5, and 10Co-Ni/ZSM-5 are 984, 904, 985, and 845 nm, respectively. These facts confirm that the surface morphology of the catalysts is not changed significantly after the impregnation of chemically doped Co metal.

3.1.3 Acidity strength of catalysts

The acid site property of catalysts was evaluated by TPD analysis using ammonia (NH_3) as the basic probe molecule. The adsorption of ammonia onto catalysts was conducted at 100 °C; therefore, it is reasonable to conclude that

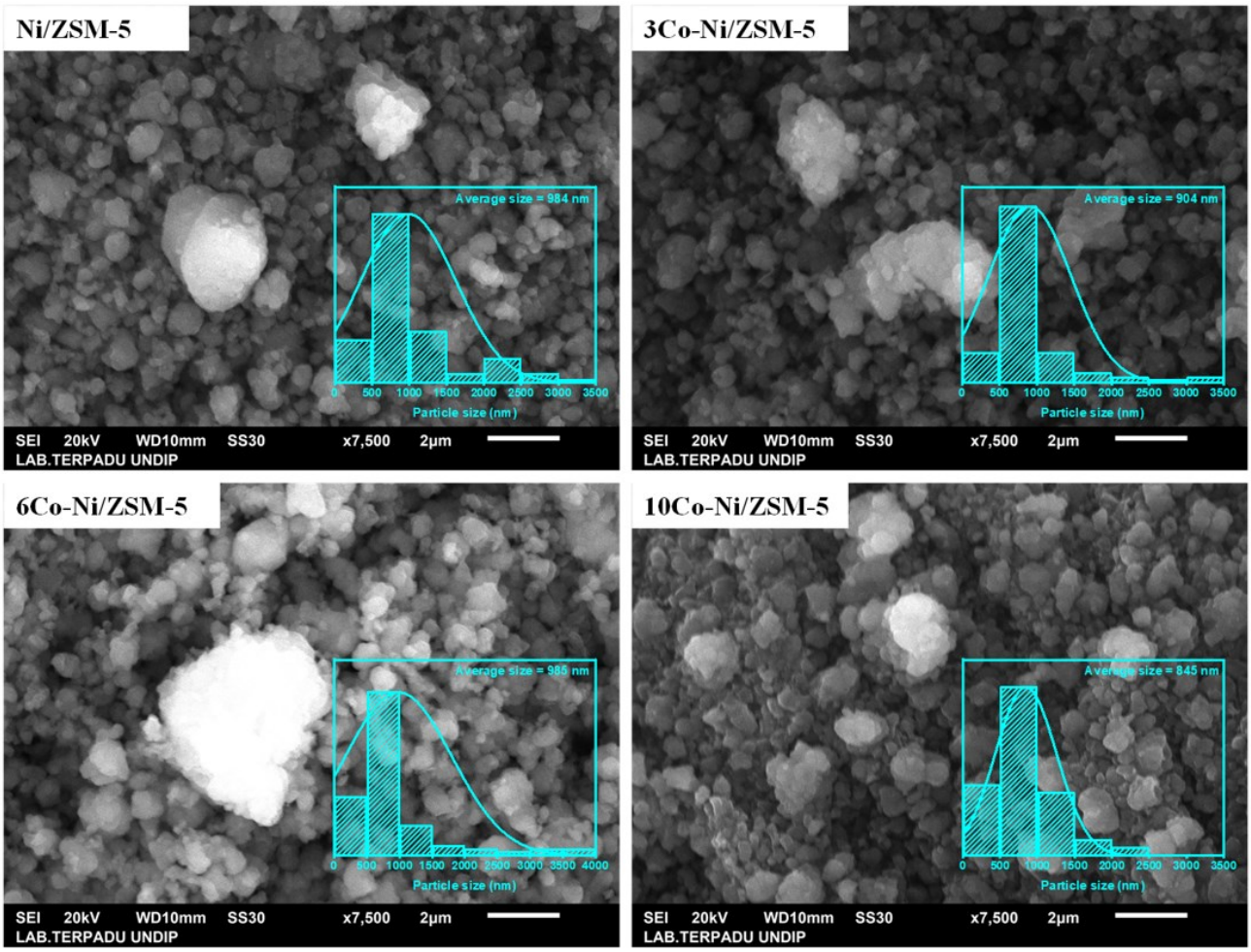

Figure 4. SEM analysis of catalysts and the particle size distribution.

the adsorbed-ammonia on catalysts were chemically adsorbed on acid sites of catalysts and the total desorbed-ammonia corresponds to the total acidity of catalysts. It is well known that the NH_3-TPD analysis allows us to identify not only the acid site amount on surface of catalysts, but also to examine the distribution of acid strength [16]. Figure 5 depicts the NH_3-TPD signals for Ni/ZSM-5, 3Co-Ni/ZSM-5, 6Co-Ni/ZSM-5, and 10Co-Ni/ZSM-5 catalysts and Table 2 shows the summary of the acid strength of catalysts. The desorption temperature of ammonia represents the acid strength of catalysts. The acid strengths from NH_3-TPD profiles are classified as weak, moderate, and strong acid sites, corresponding to the temperature desorption of NH_3 at 120–300 °C, 300–500 °C, and >500 °C, respectively [17].

Based on Figure 5 and Table 2, the acidity of catalysts is affected by the impregnation of chemically doped Co metal. As can be seen, Ni/ZSM-5 catalyst has total acidity of 449 mmol/g. The total acidity has been increased by the impregnation of chemically doped Co metal. It shows that the highest total acidity after Co impregnation was found in 10Co-Ni/ZSM-5 catalyst, which is 483 mmol/g. On the other hand, the lowest total acidity after Co impregnation was found in 10Co-Ni/ZSM-5 catalyst, which is 456 mmol/g. The chemically doping Co metal on Ni/ZSM-5 catalyst increases the total acidity of catalysts

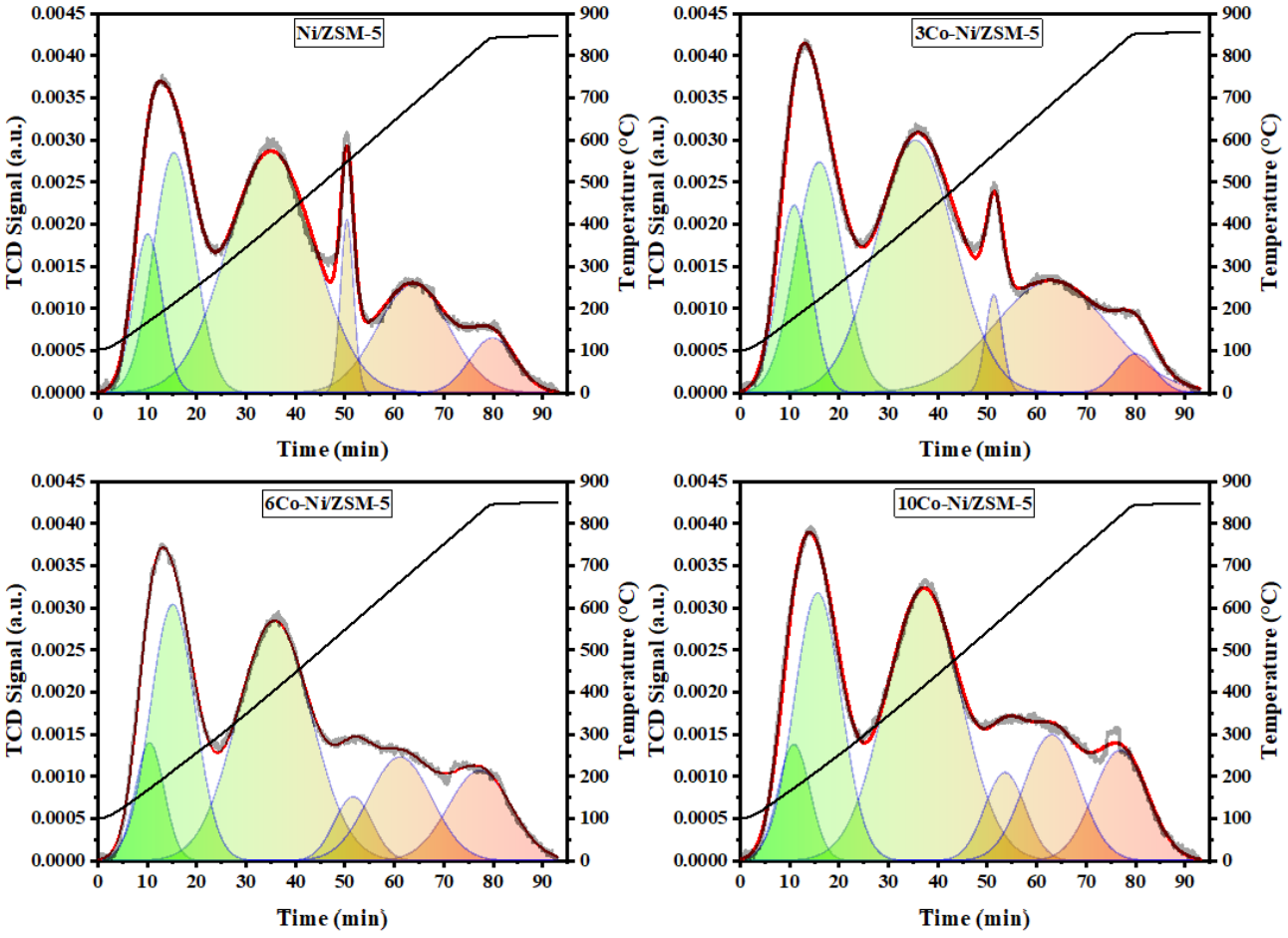

Figure 5. NH_3-TPD profile of catalysts.

Table 2. Catalysts acidity distribution.

Catalysts	Acidity (mmol/g)				Acid density (mmol/m²)
	Weak (120–300 °C)	Moderate (300–500 °C)	Strong (>500 °C)	Total	
Ni/ZSM-5	135	197	117	449	1.200
3Co-Ni/ZSM-5	152	178	142	472	1.315
6Co-Ni/ZSM-5	143	172	141	456	1.266
10Co-Ni/ZSM-5	148	185	150	483	1.329

(from 449 to 483 mmol/g). The increase in the total acidity after Co impregnation is caused by the presence of the unfilled *d* orbitals from the metal. These unfilled *d* orbitals act as the acid (Lewis) site of the catalyst [18]. This acidity increase is possibly caused by the presence of the unfilled *d* orbitals from Co metal since it is a transition metal that provides *d* orbitals which are not completely filled by electrons.

As can be seen in Figure 5, the chemically doping of Co metal on the Ni/ZSM-5 catalyst affects the profile of NH_3 desorption. It is clearly shown that the desorption peak at ~560 °C decreases gradually as the increase in the amount of Co metal doped. Moreover, the acidity strength is shifted, in which the amount of weak acidity increases, the moderate acidity decreases, and the strong acidity increases. It means that the acidity strength has been shifted from moderate acidity to weak and strong acidities because of chemically doping Ni/ZSM-5 by Co metal. This is in accordance with the previous study by Subramanian *et al.* [19] that the presence of Co metal on HZSM-5 catalyst shifts the acidity strength to weak and strong acidity. Khan *et al.* [20] also reported that this acidity peak shifting is caused by the presence of Co^{2+} which forms strong acid sites and CoO which forms weak acid sites. It was reported that the strong acidity or strong acid sites corresponds to the interaction of NH_3 with Lewis acid sites [21,22]. In the Co-based catalysts, it

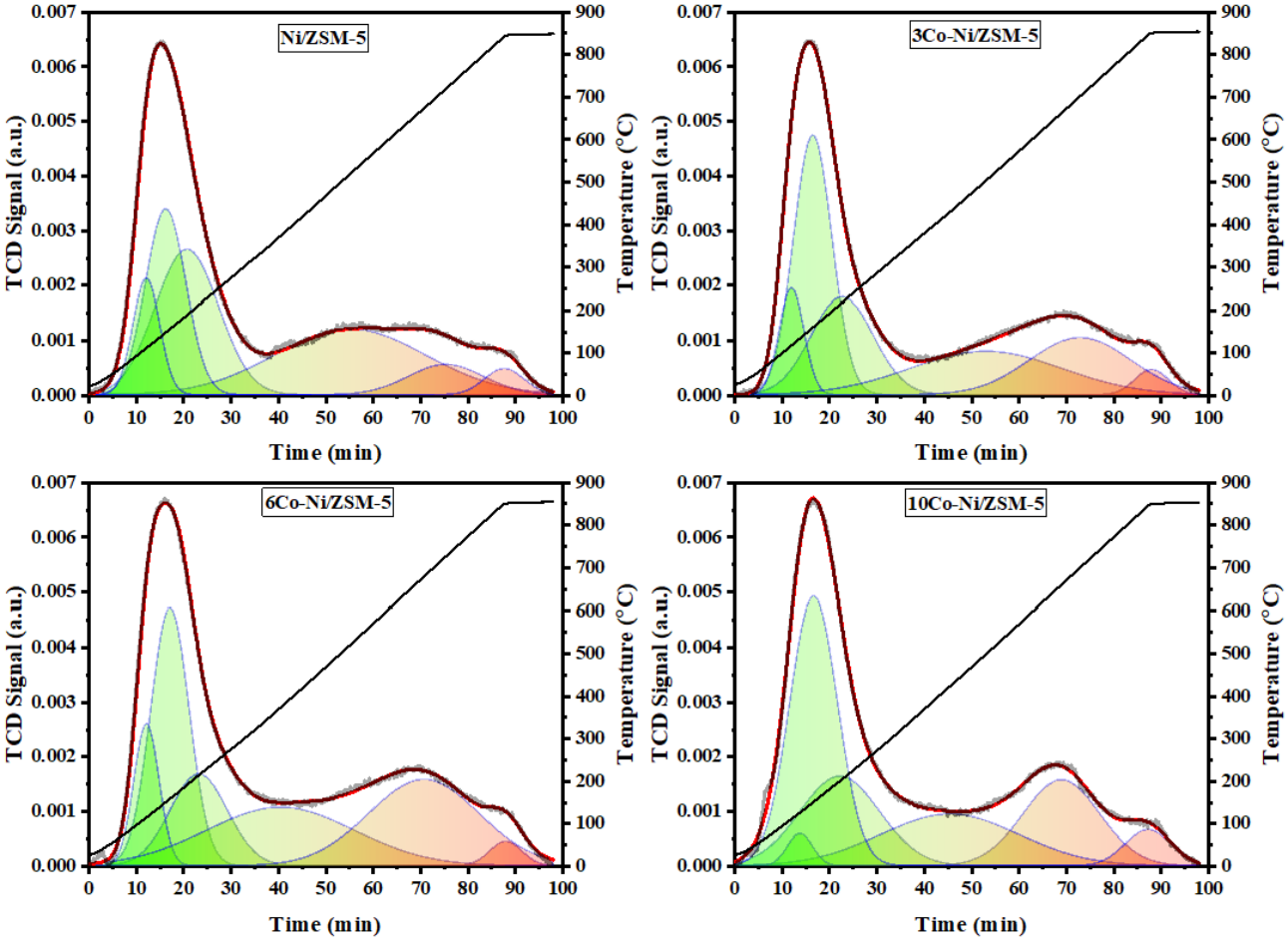

Figure 6. CO_2-TPD profile of Ni/ZSM-5, 3Co-Ni/ZSM-5, 6Co-Ni/ZSM-5, and 10Co-Ni/ZSM-5 catalysts.

Table 3. Catalysts basicity distribution.

Catalysts	Basicity (mmol/g)				Basic density (mmol/m²)
	Weak (100–160 °C)	Moderate (300–550 °C)	Strong (>600 °C)	Total	
Ni/ZSM-5	228	411	71	710	1.899
3Co-Ni/ZSM-5	274	274	145	693	1.929
6Co-Ni/ZSM-5	214	220	163	597	1.659
10Co-Ni/ZSM-5	281	292	166	739	2.033

was believed that this strong acid site is attributed to Co–O species [23,24]. Indeed, the chemically doping Co metal on Ni/ZSM-5 catalyst increases the total acidity of catalysts which caused by the presence of Co^{2+} which forms strong acid sites and CoO which forms weak acid sites which may be due to the presence of the unfilled *d* orbitals from Co metal (not completely filled by electrons) corresponding to the interaction of NH_3 with Lewis acid sites.

3.1.4 Basicity strength of catalysts

The CO_2-TPD analysis was conducted to estimate the surface basicity strength of the catalysts. Like the acidity, the basicity strengths of catalysts are classified as weak, moderate, and strong basic strengths. These classifications correspond to the temperature peaks ranging from 100 to 160 °C, 300 to 550 °C, and >600 °C, respectively [25]. In this study, the basicity strengths of catalysts were classified based on the deconvolution peaks. The CO_2-TPD profiles and the data are presented in Figure 6 and Table 3. In general, weak basic sites are assigned to surface hydroxyl groups (–OH), moderate basic sites are associated with metal-oxygen pairs, and strong basic sites are associated with low-coordinated unsaturated oxygens (O^{2-}) and electronegative anions [25].

Generally, the adjustment of zeolite-based catalysts' basicity is conducted through the ion exchanged process using alkali metals, generating the framework basicity [26]. The alkali cations, such as Li, Na, K, Rb, or Cs [27], were exchanged to the proton on the zeolite framework and play as the centre of basic site. However, the basicity of zeolite-based catalyst can be improved by the addition of metal oxide particles. As an example, Wei *et al*. [28] reported that the basicity of Zeolite 13X can be modified through the impregnation of Ni and Ce metals. Therefore, it is also necessary to investigate the effects of metal impregnation to the catalyst basicity in this study.

Based on the results of basicity characterization using CO_2-TPD method, it was found that the addition of Co metal affects slightly the basicity of the catalysts, as shown in Figure 6 and Table 3. It is shown that the basicity of the Ni/ZSM-5 catalyst is 710 mmol/g. The basicity of the catalysts then decreases slightly as the increase in the amount of Co metal addition and increased slightly to 739 mmol/g at doping 10 wt% Co. It indicates that the addition of Co metal influences only slightly the basicity of the catalysts. The addition of Co metal on the Ni/ZSM-5 catalyst may create strong basic sites due to the presence of low-coordinated unsaturated oxygens (O^{2-}) in the catalysts [25,29,30]. Indeed, the chemically doping Co metal on Ni/ZSM-5 catalyst increases slightly or not significantly changes the total basicity of catalysts.

3.2 Catalysts Performance Towards Palm Oil Cracking

The performance of the synthesized catalysts was evaluated through cracking process of palm oil to liquid fuels. The fixed bed continuous reactor was at 450 °C with a WHSV of 0.365 min^{-1}. The liquid fuel product was collected, and the coke analysis is then deeply investigated using TGA method and discussed in the next section. The yield of liquid product is presented in Figure 7. As can be seen, the yield

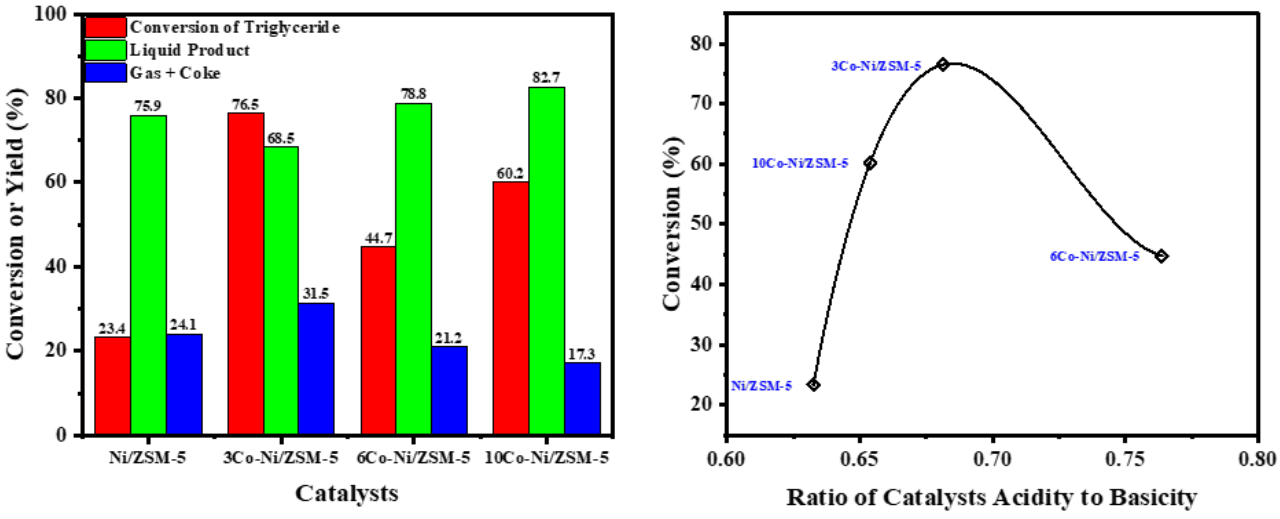

Figure 7. Catalysts performance of palm oil conversion and the effect of the ratio of catalysts acidity to basicity on palm oil conversion.

of liquid product of Ni/ZSM-5, 3Co-Ni/ZSM-5, 6Co-Ni/ZSM-5, and 10Co-Ni/ZSM-5 are 75.9, 68.5, 78.8, and 82.7%, respectively.

In order to investigate the triglyceride conversion and the functional groups in the liquid product, the liquid product was analyzed using FT-IR analysis. The FT-IR spectra of the palm oil and the liquid fuels are presented in Figure 8. It can be seen that the main functional groups in the liquid fuels product are ester, carboxylic acid, and hydrocarbon. In addition, it is shown that some peaks decrease, and some new peaks also appear. Based on Figure 8, the FT-IR spectra of palm oil and liquid products show absorption bands at 2922 cm^{-1} and 2853 cm^{-1} which are attributed to the asymmetric and symmetric stretching C−H from methylene group [31,32]. These peaks are associated to the absorption band at 720 cm^{-1}, which is attributed to the rocking vibration of C−H from methylene group [32]. Furthermore, the absorption bands at 1460 cm^{-1} and 1377 cm^{-1} are attributed to the asymmetric bend and symmetric bend (umbrella bending mode) of C−H form methyl. The appearance of these absorption peaks indicates that the palm oil and liquid fuels have hydrocarbon chain. In the palm oil, it is found that there is hydrocarbon chain of the fatty acid structure, and also the carbonyl (C=O) structure at 1745 cm^{-1}. This peak is attributed to the stretching vibration of the carbonyl group from ester structure. It can be indicated the appearance of the associated peak at 1161 cm^{-1}, which attributed to the vibration of C−O−C bond.

It can be seen that the liquid products have some new absorption bands at wavenumber of 1710 and 942 cm^{-1}, which are assigned to the stretching vibration of C=O from carboxylic acid and the vibration of O−H, respectively. It is noted that the stretching vibration of carbonyl structure (C=O) has been shifted from 1745 cm^{-1} in palm oil to 1710 cm^{-1} in the liquid products. It means that the carbonyl structure from ester structure has been converted to carboxylic acid. It is proven by the decrease in the absorption band at 1161 cm^{-1} (vibration of C−O−C). It means that the triglyceride structure is broken, producing carboxylic acid as the intermediate product. Using the area of the absorption peak at 1745 cm^{-1}, the conversion of ester bond, which can be assigned to the conversion of triglyceride, can be calculated. The conversion of triglyceride as the function of catalysts acidity, represented as ratio of catalysts acidity and basicity, is presented in Figure 7. It can be seen that the conversion of triglyceride on the modified Ni/ZSM-5 catalysts is higher than pristine Ni/ZSM-5 catalyst. In addition, the triglyceride conversion increases as the increase in the ratio of catalysts acidity and basicity which means that the conversion is related to the catalysts' acidity. The increase in the catalysts' acidity in bimetallic catalysts (Co-Ni/ZSM-5) increase the active sites that can be effectively reached by the reactant molecules (triglyceride) than the unimetal catalyst (Ni/ZSM-5). Therefore, it can be concluded that the only chemically addition of Co metal on the Ni/ZSM-5 catalyst increases the conversion of palm oil because of increasing the catalysts' acidity, which is confirmed by NH_3-TPD characterization results.

3.3 Liquid Fuels Distribution

Batch distillation was applied to determine the yield of gasoline (≤205 °C), kerosene (205-

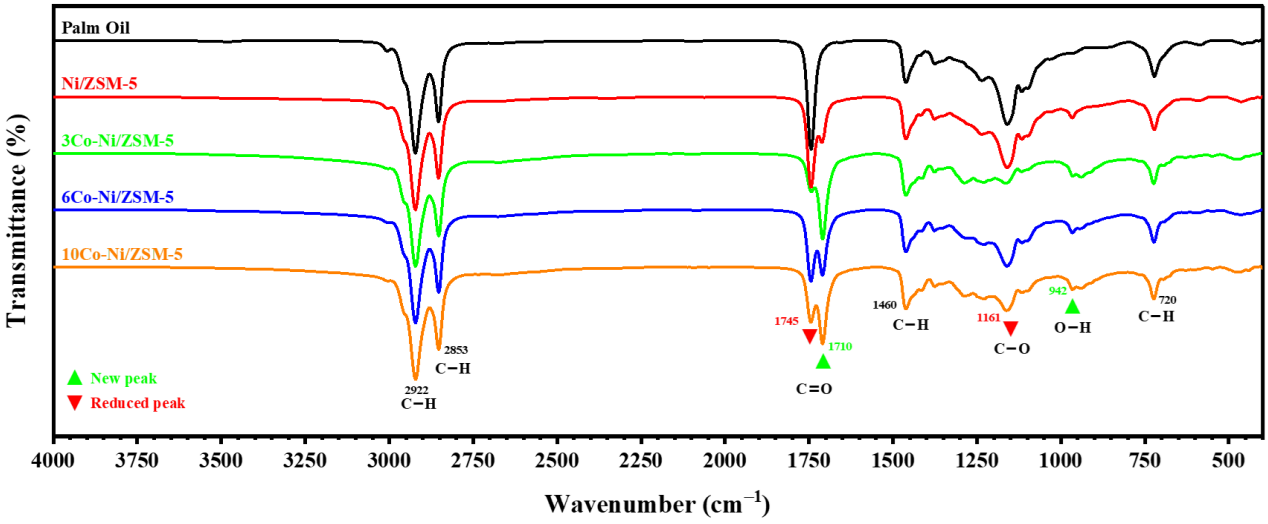

Figure 8. FT-IR spectra of palm oil and liquid fuels.

310 °C), and diesel (310-370 °C) fraction in the liquid products. The liquid products distribution is presented in Figure 9. As can be seen, Ni/ZSM-5, 3Co-Ni/ZSM-5, 6Co-Ni/ZSM-5, and 10Co-Ni/HSM-5 gives the yield of gasoline of 0.15%, 2.61%, 0.43% and 0.75%, respectively. The higher fraction (kerosene) is obtained in a higher number than gasoline fraction which is 0.27%, 4.38%, 1.19% and 3.37% for Ni/ZSM-5, 3Co-Ni/ZSM-5, 6Co-Ni/ZSM-5, and 10Co-Ni/HSM-5, respectively. The highest component is diesel fraction which is produced at 52.02%, 61.72%, 77.36%, and 71.31% by Ni/ZSM-5, 3Co-Ni/ZSM-5, 6Co-Ni/ZSM-5, and 10Co-Ni/HSM-5, respectively. From Figure 9, the amount of gasoline in the liquid product markedly increases as the increase in conversion. In addition, the yield of kerosene increases in a sigmoidal manner as the increase in conversion. On the other hand, the yield of diesel increases as the increase in conversion up to ~45% and then decreases at further increase in conversion.

The yield of diesel decreases at a high conversion, means that the component of liquid products is shifted from heavy fraction to light fraction at high conversion of palm oil. At high conversion, the liquid product is shifted from diesel to kerosene and gasoline, because of the shifting of acidity strength of catalysts. The only chemically addition of Co metal on the Ni/HZSM-5 catalyst resulted in a shift in the acid sites which was previously dominant on the moderate acid sites to strong and weak acid sites. Subramanian *et al*. [19] reported that the presence of strong acid sites on the Co/HZSM-5 catalyst tends to direct the cracking selectivity of C_5–C_{12} hydrocarbon chains, while the presence of weak acid sites on the Co/HZSM-5 catalyst increases the selectivi-

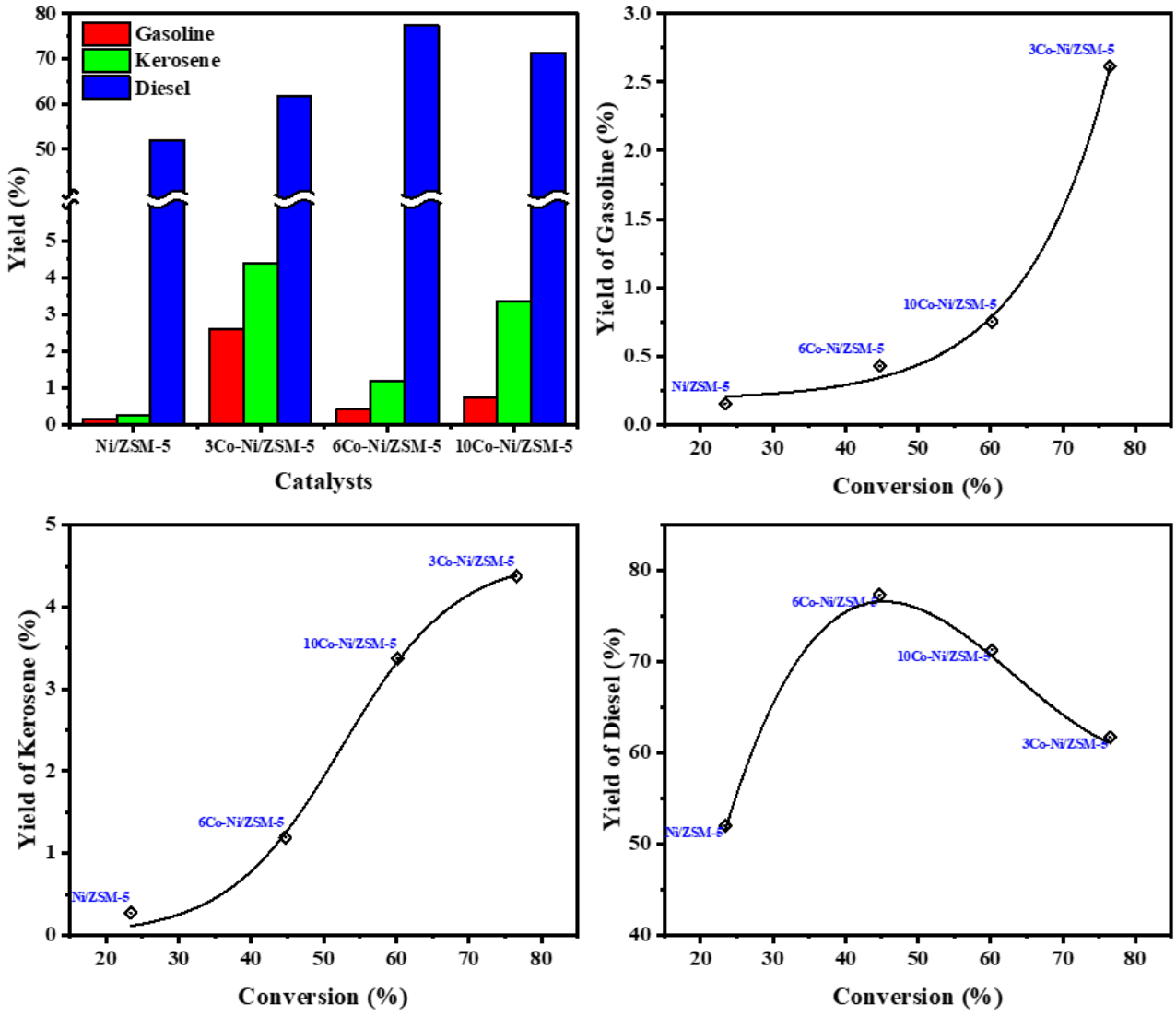

Figure 9. Liquid product distribution as affected by catalyst and triglyceride conversion.

ty of C_5–C_8 hydrocarbon chain cracking. This is consistent with this results research where the 3Co-Ni/HZSM-5 catalyst with the highest number of weak acid sites produced the highest gasoline compared to other Co-Ni/HZSM-5 catalysts (see Table 2).

3.4 Coke Formation Analysis

In order to estimate the amount of carbon-coke on the spent catalysts, the spent catalysts were analyzed using TGA with mixed nitrogen-oxygen gas method. Figure 10 depicts the results of TG, DTG, and DSC curves of all spent catalysts. As can be seen, the TG curves mainly consist of three different weight loss steps. A slight of small weight loss before 200 °C is attributed to the evaporation of water molecules that was physically adsorbed. The second and third weight loss at 200–470 °C and >470°C are attributed to the combustion of amorphous carbon and graphitic carbon the spent catalysts, respectively [33]. The total amount of the deposited carbon on Ni/ZSM-5, 3Co-Ni/ZSM-5, 6Co-Ni/ZSM-5, and 10Co-Ni/HSM-5 are 36.22%, 35.91%, 24.42%, and 33.15%, respectively. In addition, all catalysts produce amorphous and graphitic carbons. Amorphous or soft carbon-coke is basically produced by porous materials. This kind of deposited carbon is easier to be decomposed than graphitic or hard carbon-coke. It can be seen that the soft carbon-coke is rapidly decomposed, indicated by the rapid weight loss (Figure 10(A)) or high decomposition rate (Figure 10(B)). A fast decomposition or combustion in TGA is indicated by a high-narrow DTG signal. On the other hand, the hard carbon-coke is difficult to be decomposed. It can be seen that the decomposition rate or DTG signal of hard carbon-coke is broad. The DSC signal also shows a broad exothermic peak for hard carbon-coke combustion. It indicates that the hard carbon-coke is difficult to be decomposed.

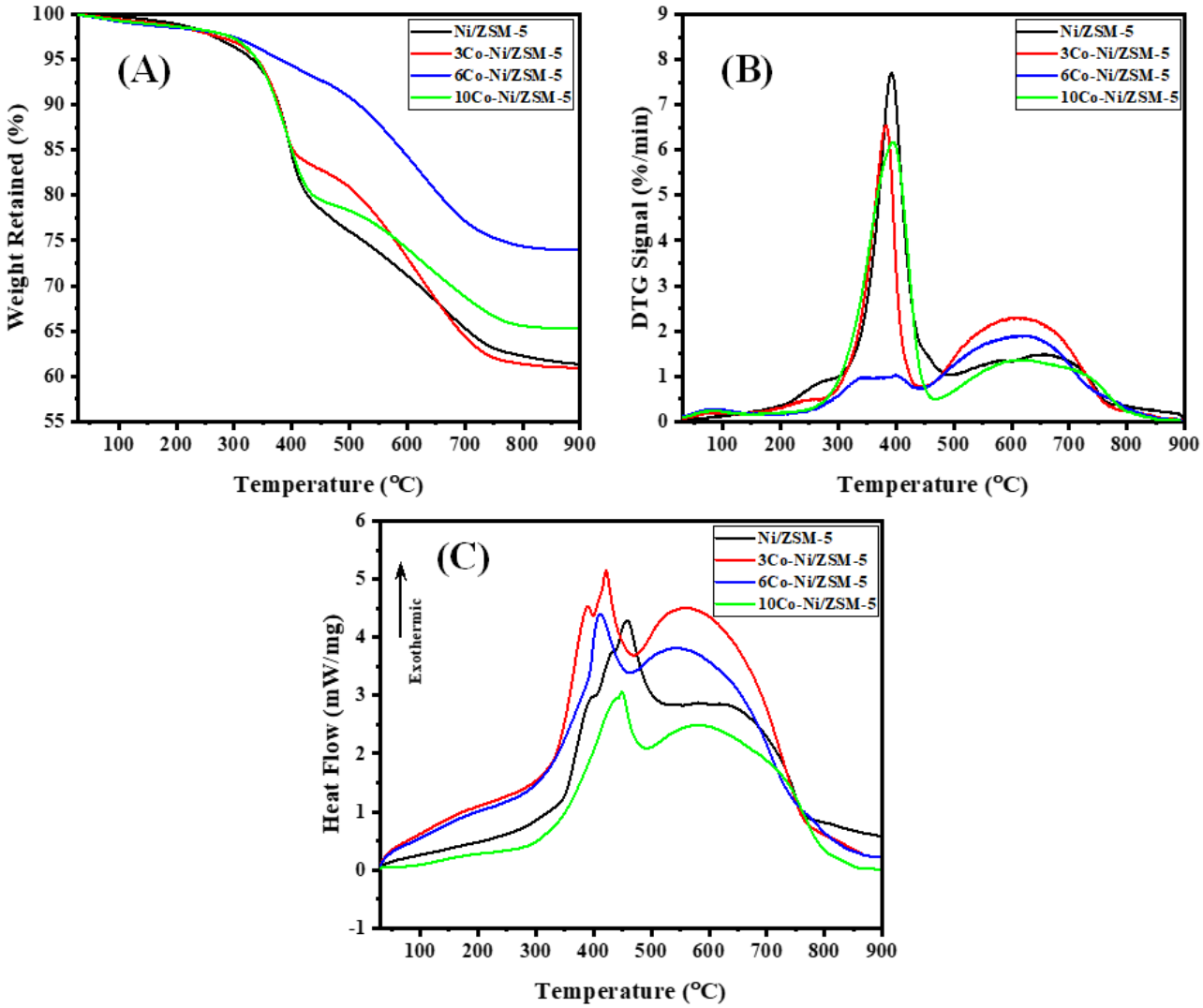

Figure 10. Coke analysis using (A) thermal gravimetry (TG), (D) DTG, and (C) DSC.

If the formation of coke is occurred, the catalyst will be deactivated so that the catalysts active sites decrease which can slow down the reaction. In general, partial closing of the catalyst pores by carbon-coke can negatively affect the performance of the catalyst. In this study, increasing the concentration of Co promoter on the chemically doped catalyst resulted in increasing the total acidity of the catalyst (Figure 5, Table 2). At excessive levels of acidity, aromatic products will undergo polymerization into larger hydrocarbon molecules resulting in a faster rate of carbon-coke formation. As a result, the catalyst pores are covered by carbon-coke so that the reactants did not undergo a cracking reaction because they could not enter the pore surface. These coke molecules block the diffusion process of the reactant molecules to the acid sites centre of the catalysts. On the other hand, the active centre can no longer be an acid active centre because it has bound carbon-coke.

Based on the TGA results, the addition of Co metal decreases the possibility of carbon-coke formation, compared to Ni/ZSM-5 catalyst, in which the Ni/ZSM-5 catalyst has the highest carbon-coke (36.22%) formation. It is possible, since Ni metal has high affinity of carbon-coke formation [12]. The deficiency of Ni metal which has a high carbon-coke yield can be suppressed by the metal promoter properties of Co metal which can inhibit carbon-coke formation [34]. The ability of metal Co to inhibit the rate of carbon-coke formation is due to the presence of metal oxides, which can be CoO and Co_3O_4 [35]. Furthermore, the 3Co-Ni/ZSM-5 and 10Co-Ni/ZSM-5 catalysts have a higher yield of carbon-coke than the 6Co-Ni/ZSM-5 catalyst. This phenomenon is related to the acidity value of the catalyst, where in general a high level of acidity of the catalyst will be directly proportional to the formation of high carbon-coke as well [36]. This statement is in accordance with the results of the study, namely the high acidity values of the catalysts 3Co-Ni/HZSM-5 and 10Co-Ni/HZSM-5 which resulted in the formation of high carbon-coke yields as well.

The addition of Co on Ni/ZSM-5 catalyst decreases the coke formation. It was reported by Charisiou *et al*. [37] that strong base sites play a major role in maintaining catalyst activity and stability. They reported that, when the number of strong base sites and total basicity is excessive, the catalyst will be more easily deactivated, conversely, if the sites are strong base and the total basicity is not too large, it will maintain its stability and activity longer. Accordantly, Zhang *et al*. [38] also reported that, in excess of the amount of catalysts' basicity, the activity of catalysts will decrease due to the increase in the rate of carbon-coke formation. This phenomenon is in accordance with the results of this study which is shown that the lowest basicity (6Co-Ni/ZSM-5) has the lowest deposited carbon-coke.

4. Conclusion

The simultaneous cracking-deoxygenation of palm oil to biofuels was studied using ZSM-5 derived-catalysts (Ni/ZSM-5, 3Co-Ni/ZSM-5, 6Co-Ni/ZSM-5, 10Co-Ni/ZSM-5). Only chemically doping Co metal on the Ni/ZSM-5 increased the catalysts acidity and decreased slightly the catalysts basicity which is also increased the performance of cracking-deoxygenation reaction of palm oil to biofuels. Moreover, the only chemically addition of Co metal on the Ni/ZSM-5 catalyst could decrease the carbon-coke formation, because of lower basicity of the catalyst. The lowest carbon-coke formation was found at 6Co-Ni/ZSM-5 catalyst due to the lowest basicity strength. However, the most effective catalyst for biofuels production from palm oil cracking was 3Co-Ni/ZSM-5 with highest conversion and biofuels yield.

Acknowledgement

Authors would like to express their sincere gratitude to the *Lembaga Penelitian dan Pengabdian kepada Masyarakat* (LPPM) Universitas Diponegoro for the financial support through the research project of *Riset Publikasi Internasional* (RPI) with grant number: 569-132/UN7.D2/PP/VII/2022

CRediT Author Statement

Author Contributions: I. Istadi: Conceptualization, Methodology, Investigation, Resources, Data Curation, Writing, Review and Editing, Supervision; T. Riyanto: Conceptualization, Methodology, Formal Analysis, Data Curation, Writing Draft Preparation, Visualization, Project Administration; D.D. Agggoro: Resources, Validation, Writing, Review and Editing, Data Curation; C.S. Pramana: Experimental Investigation; A.R. Ramadhani: Experimental Investigation. All authors have read and agreed to the published version of the manuscript.

References

[1] Baharudin, K.B., Abdullah, N., Taufiq-Yap, Y.H., Derawi, D. (2020). Renewable diesel via solventless and hydrogen-free catalytic deoxygenation of palm fatty acid distillate. *Journal of Cleaner Production*, 274, 122850. DOI: 10.1016/j.jclepro.2020.122850.

[2] Knothe, G. (2010). Biodiesel: Current Trends and Properties. *Topics in Catalysis*, 53(11–12), 714–720. DOI: 10.1007/s11244-010-9457-0.

[3] Adira Wan Khalit, W.N., Marliza, T.S., Asikin-Mijan, N., Gamal, M.S., Saiman, M.I., Ibrahim, M.L., Taufiq-Yap, Y.H. (2020). Development of bimetallic nickel-based catalysts supported on activated carbon for green fuel production. *RSC Advances*, 10(61), 37218–37232. DOI: 10.1039/D0RA06302A.

[4] Asikin-Mijan, N., Lee, H.V., Taufiq-Yap, Y.H., Juan, J.C., Rahman, N.A. (2016). Pyrolytic–deoxygenation of triglyceride via natural waste shell derived $Ca(OH)_2$ nanocatalyst. *Journal of Analytical and Applied Pyrolysis*, 117, 46–55. DOI: 10.1016/j.jaap.2015.12.017.

[5] Gamal, M.S., Asikin-Mijan, N., Khalit, W.N.A.W., Arumugam, M., Izham, S.M., Taufiq-Yap, Y.H. (2020). Effective catalytic deoxygenation of palm fatty acid distillate for green diesel production under hydrogen-free atmosphere over bimetallic catalyst CoMo supported on activated carbon. *Fuel Processing Technology*, 208, 106519. DOI: 10.1016/j.fuproc.2020.106519.

[6] Riyanto, T., Istadi, I., Buchori, L., Anggoro, D.D., Dani Nandiyanto, A.B. (2020). Plasma-Assisted Catalytic Cracking as an Advanced Process for Vegetable Oils Conversion to Biofuels: A Mini Review. *Industrial & Engineering Chemistry Research*, 59(40), 17632–17652. DOI: 10.1021/acs.iecr.0c03253.

[7] Buzetzki, E., Sidorová, K., Cvengrošová, Z., Kaszonyi, A., Cvengroš, J. (2011). The influence of zeolite catalysts on the products of rapeseed oil cracking. *Fuel Processing Technology*, 92(8), 1623–1631. DOI: 10.1016/j.fuproc.2011.04.009.

[8] Ishihara, A., Tsukamoto, T., Hashimoto, T., Nasu, H. (2018). Catalytic cracking of soybean oil by ZSM-5 zeolite-containing silica-aluminas with three layered micro-meso-meso-structure. *Catalysis Today*, 303, 123–129. DOI: 10.1016/j.cattod.2017.09.033.

[9] Gurdeep Singh, H.K., Yusup, S., Quitain, A.T., Abdullah, B., Ameen, M., Sasaki, M., Kida, T., Cheah, K.W. (2020). Biogasoline production from linoleic acid via catalytic cracking over nickel and copper-doped ZSM-5 catalysts. *Environmental Research*, 186, 109616. DOI: 10.1016/j.envres.2020.109616.

[10] Istadi, I., Riyanto, T., Buchori, L., Anggoro, D.D., Gilbert, G., Meiranti, K.A., Khofiyanida, E. (2020). Enhancing Brønsted and Lewis Acid Sites of the Utilized Spent RFCC Catalyst Waste for the Continuous Cracking Process of Palm Oil to Biofuels. *Industrial & Engineering Chemistry Research*, 59(20), 9459–9468. DOI: 10.1021/acs.iecr.0c01061.

[11] Istadi, I., Riyanto, T., Buchori, L., Anggoro, D.D., Pakpahan, A.W.S., Pakpahan, A.J. (2021). Biofuels Production from Catalytic Cracking of Palm Oil Using Modified HY Zeolite Catalysts over A Continuous Fixed Bed Catalytic Reactor. *International Journal of Renewable Energy Development*, 10(1), 149–156. DOI: 10.14710/ijred.2021.33281.

[12] Riyanto, T., Istadi, I., Jongsomjit, B., Anggoro, D.D., Pratama, A.A., Faris, M.A. Al (2021). Improved Brønsted to Lewis (B/L) Ratio of Co- and Mo-Impregnated ZSM-5 Catalysts for Palm Oil Conversion to Hydrocarbon-Rich Biofuels. *Catalysts*, 11(11), 1286. DOI: 10.3390/catal11111286.

[13] Botas, J.A., Serrano, D.P., García, A., de Vicente, J., Ramos, R. (2012). Catalytic conversion of rapeseed oil into raw chemicals and fuels over Ni- and Mo-modified nanocrystalline ZSM-5 zeolite. *Catalysis Today*, 195(1), 59–70. DOI: 10.1016/j.cattod.2012.04.061.

[14] Haji Morni, N.A., Yeung, C.M., Tian, H., Yang, Y., Phusunti, N., Abu Bakar, M.S., Azad, A.K. (2021). Catalytic fast Co-Pyrolysis of sewage sludge−sawdust using mixed metal oxides modified with ZSM-5 catalysts on dual-catalysts for product upgrading. *Journal of the Energy Institute*, 94, 387–397. DOI: 10.1016/j.joei.2020.10.005.

[15] Thommes, M., Kaneko, K., Neimark, A. V., Olivier, J.P., Rodriguez-Reinoso, F., Rouquerol, J., Sing, K.S.W. (2015). Physisorption of gases, with special reference to the evaluation of surface area and pore size distribution (IUPAC Technical Report). *Pure and Applied Chemistry*, 87(9–10), 1051–1069. DOI: 10.1515/pac-2014-1117.

[16] Pietrowski, M., Zieliński, M., Alwin, E., Gulaczyk, I., Przekop, R.E., Wojciechowska, M. (2019). Cobalt-doped magnesium fluoride as a support for platinum catalysts: The correlation of surface acidity with hydrogenation activity. *Journal of Catalysis*, 378, 298–311. DOI: 10.1016/j.jcat.2019.09.001.

[17] Musa, M.L., Mat, R., Abdullah, T.A.T. (2018). Catalytic Conversion of Residual Palm Oil in Spent Bleaching Earth (SBE) by HZSM-5 Zeolite based-Catalysts. *Bulletin of Chemical Reaction Engineering & Catalysis*, 13(3), 456–465. DOI: 10.9767/bcrec.13.3.1929.456-465.

[18] Anggoro, D.D., Hidayati, N., Buchori, L., Mundriyastutik, Y. (2016). Effect of Co and Mo Loading by Impregnation and Ion Exchange Methods on Morphological Properties of Zeolite Y Catalyst. *Bulletin of Chemical Reaction Engineering & Catalysis*, 11(1), 75–83. DOI: 10.9767/bcrec.11.1.418.75-83.

[19] Subramanian, V., Zholobenko, V.L., Cheng, K., Lancelot, C., Heyte, S., Thuriot, J., Paul, S., Ordomsky, V. V., Khodakov, A.Y. (2016). The Role of Steric Effects and Acidity in the Direct Synthesis of iso -Paraffins from Syngas on Cobalt Zeolite Catalysts. *ChemCatChem*, 8(2), 380–389. DOI: 10.1002/cctc.201500777.

[20] Khan, N.A., Kennedy, E.M., Dlugogorski, B.Z., Adesina, A.A., Stockenhuber, M. (2017). Cobalt Species Active for Nitrous Oxide (N_2O) Decomposition within a Temperature Range of 300–600°C. *Australian Journal of Chemistry*, 70(10), 1138. DOI: 10.1071/CH17172.

[21] Zheng, Y., Guo, Y., Wang, J., Luo, L., Zhu, T. (2021). Ca Doping Effect on the Competition of NH_3–SCR and NH_3 Oxidation Reactions over Vanadium-Based Catalysts. *The Journal of Physical Chemistry C*, 125(11), 6128–6136. DOI: 10.1021/acs.jpcc.1c00677.

[22] Putluru, S.S.R., Jensen, A.D., Riisager, A., Fehrmann, R. (2011). Alkali Resistant Fe-Zeolite Catalysts for SCR of NO with NH_3 in Flue Gases. *Topics in Catalysis*, 54(16–18), 1286–1292. DOI: 10.1007/s11244-011-9750-6.

[23] Sadek, R., Chalupka, K.A., Mierczynski, P., Rynkowski, J., Gurgul, J., Dzwigaj, S. (2019). Cobalt Based Catalysts Supported on Two Kinds of Beta Zeolite for Application in Fischer-Tropsch Synthesis. *Catalysts*, 9(6), 497. DOI: 10.3390/catal9060497.

[24] Tišler, Z., Klegová, A., Svobodová, E., Šafář, J., Strejcová, K., Kohout, J., Šlang, S., Pacultová, K., Rodríguez-Padrón, D., Bulánek, R. (2020). Cobalt Based Catalysts on Alkali-Activated Zeolite Foams for N_2O Decomposition. *Catalysts*, 10(12), 1398. DOI: 10.3390/catal10121398.

[25] Ezeh, C.I., Yang, X., He, J., Snape, C., Cheng, X.M. (2018). Correlating ultrasonic impulse and addition of ZnO promoter with CO_2 conversion and methanol selectivity of CuO/ZrO_2 catalysts. *Ultrasonics Sonochemistry*, 42, 48–56. DOI: 10.1016/j.ultsonch.2017.11.013.

[26] Busca, G. (2017). Acidity and basicity of zeolites: A fundamental approach. *Microporous and Mesoporous Materials*, 254, 3–16. DOI: 10.1016/j.micromeso.2017.04.007.

[27] Mignon, P., Geerlings, P., Schoonheydt, R. (2006). Understanding the Concept of Basicity in Zeolites. A DFT Study of the Methylation of Al−O−Si Bridging Oxygen Atoms. *The Journal of Physical Chemistry B*, 110(49), 24947–24954. DOI: 10.1021/jp064762d.

[28] Wei, L., Grénman, H., Haije, W., Kumar, N., Aho, A., Eränen, K., Wei, L., de Jong, W. (2021). Sub-nanometer ceria-promoted Ni 13X zeolite catalyst for CO_2 methanation. *Applied Catalysis A: General*, 612, 118012. DOI: 10.1016/j.apcata.2021.118012.

[29] Efremova, A., Szenti, I., Kiss, J., Szamosvölgyi, Á., Sápi, A., Baán, K., Olivi, L., Varga, G., Fogarassy, Z., Pécz, B., Kukovecz, Á., Kónya, Z. (2022). Nature of the Pt-Cobalt-Oxide surface interaction and its role in the CO_2 Methanation. *Applied Surface Science*, 571, 151326. DOI: 10.1016/j.apsusc.2021.151326.

[30] Fiorenza, R., Bellardita, M., Balsamo, S.A., Spitaleri, L., Gulino, A., Condorelli, M., D'Urso, L., Scirè, S., Palmisano, L. (2022). A solar photothermocatalytic approach for the CO_2 conversion: Investigation of different synergisms on CoO-CuO/brookite TiO_2-CeO_2 catalysts. *Chemical Engineering Journal*, 428, 131249. DOI: 10.1016/j.cej.2021.131249.

[31] Coates, J. (2006). Interpretation of Infrared Spectra, A Practical Approach. In: *Encyclopedia of Analytical Chemistry*. Chichester, UK: John Wiley & Sons, LtdDOI: 10.1002/9780470027318.a5606.

[32] Smith, B.C. (1998). *Infrared Spectral Interpretation: A Systematic Approach*. Boca Raton, USA: CRC Press.

[33] Mhadmhan, S., Natewong, P., Prasongthum, N., Samart, C., Reubroycharoen, P. (2018). Investigation of Ni/SiO_2 Fiber Catalysts Prepared by Different Methods on Hydrogen Production from Ethanol Steam Reforming. *Catalysts*, 8(8), 319. DOI: 10.3390/catal8080319.

[34] Hou, Y., Nagamatsu, S., Asakura, K., Fukuoka, A., Kobayashi, H. (2018). Trace monoatomically dispersed rhodium on zeolite-supported cobalt catalyst for the efficient methane oxidation. *Communications Chemistry*, 1(1), 41. DOI: 10.1038/s42004-018-0044-9.

[35] Iliopoulou, E.F., Stefanidis, S.D., Kalogiannis, K.G., Delimitis, A., Lappas, A.A., Triantafyllidis, K.S. (2012). Catalytic upgrading of biomass pyrolysis vapors using transition metal-modified ZSM-5 zeolite. *Applied Catalysis B: Environmental*, 127, 281–290. DOI: 10.1016/j.apcatb.2012.08.030.

[36] Huang, J., Jiang, Y., Marthala, V.R.R., Bressel, A., Frey, J., Hunger, M. (2009). Effect of pore size and acidity on the coke formation during ethylbenzene conversion on zeolite catalysts. *Journal of Catalysis*, 263(2), 277–283. DOI: 10.1016/j.jcat.2009.02.019.

[37] Charisiou, N.D., Siakavelas, G., Tzounis, L., Sebastian, V., Monzon, A., Baker, M.A., Hinder, S.J., Polychronopoulou, K., Yentekakis, I.V., Goula, M.A. (2018). An in depth investigation of deactivation through carbon formation during the biogas dry reforming reaction for Ni supported on modified with CeO_2 and La_2O_3 zirconia catalysts. *International Journal of Hydrogen Energy*, 43(41), 18955–18976. DOI: 10.1016/j.ijhydene.2018.08.074.

[38] Zhang, Z., Zhang, X., Zhang, L., Wang, Y., Li, X., Zhang, S., Liu, Q., Wei, T., Gao, G., Hu, X. (2020). Steam reforming of guaiacol over Ni/SiO_2 catalyst modified with basic oxides: Impacts of alkalinity on properties of coke. *Energy Conversion and Management*, 205, 112301. DOI: 10.1016/j.enconman.2019.112301.